

Meta-Optimization for Higher Model Generalizability in Single-Image Depth Prediction

Cho-Ying Wu Yiqi Zhong Junying Wang Ulrich Neumann

University of Southern California

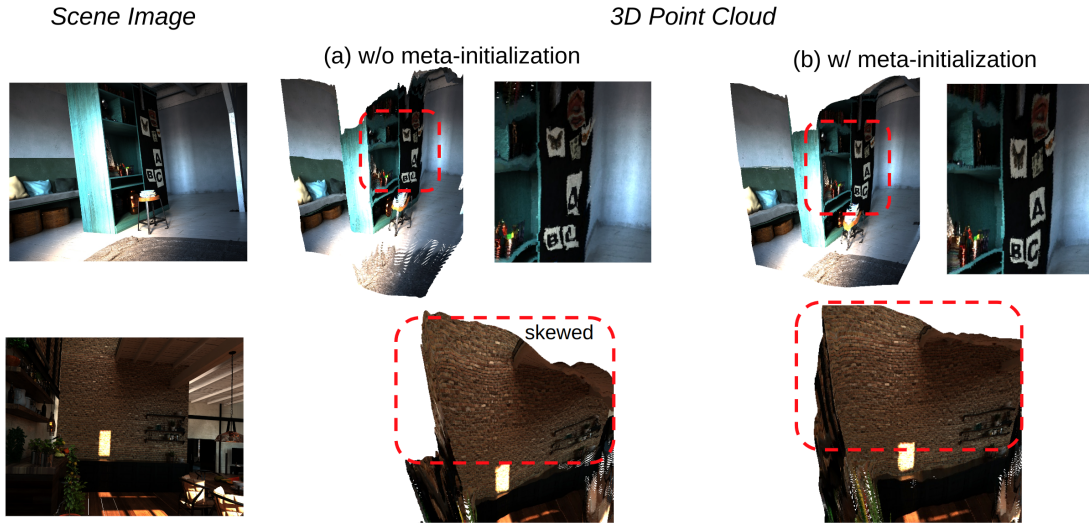


Figure 1. **Geometry structure comparison in 3D point cloud view.** We back-project the predicted depth maps from images into textured 3D point cloud to show the geometry. The proposed Meta-Initialization has better domain generalizability that leads to more accurate depth prediction hence better 3D structures. (zoom in for the best view).

Abstract

Model generalizability to unseen datasets, concerned with in-the-wild robustness, is less studied for indoor single-image depth prediction. We leverage gradient-based meta-learning for higher generalizability on zero-shot cross-dataset inference. Unlike the most-studied image classification in meta-learning, depth is pixel-level continuous range values, and mappings from each image to depth vary widely across environments. Thus no explicit task boundaries exist. We instead propose fine-grained task that treats each RGB-D pair as a task in our meta-optimization. We first show meta-learning on limited data induces much better prior (max +29.4%). Using meta-learned weights as initialization for following supervised learning, without involving extra data or information, it consistently outperforms baselines without the method. Compared to most indoor-depth methods that only train/ test on a single dataset, we propose zero-shot cross-dataset protocols, closely evaluate robustness, and show consistently higher generalizability and accuracy by our meta-initialization. The work at the intersection of depth and meta-learning potentially drives both research streams to step closer to practical use.

1. Introduction

Much research attempts to learn geometry of scenes, representing in depth maps, from single images to fulfill physical indoor applications with depth such as collision detection [23, 52, 85], robot navigation [35, 72, 73], grasping [35, 67, 77], human verification or interaction [80, 81, 84, 88, 90] or it benefits learning good 3D representations for novel view synthesis using depth supervision [17, 64] with on-the-fly single-image depth estimation. However, learning precise image-to-depth mappings is challenging due to domain gaps. A model weakly capturing such relations may produce vague depth maps or even cannot identify near and far fields.

An intuitive solution is to learn from large-scale data or employ side information such as normal [61, 62, 94], or pre-trained knowledge as guidance [89]. However, they require extra information burdens. Without those resources when training on data of limited appearance and depth variation, referring to *scene variety*, with an extreme case that only sparse and irrelevant RGB-D pairs are available, networks can barely learn a valid image-to-depth mapping (Fig. 5).

Inspired by meta-learning’s advantages of domain gener-

alizability, training robust generalization models to achieve better results on unknown domains, usually learned from limited-source data [21, 22, 34, 54], we pioneer to dig into how meta-learning applies to single-image depth prediction. The commonly-used meta-learning problem setup follows the context of few-shot multitask settings, where a task represents a distribution to sample data from, and most tasks are designed for image classification [34]. Unlike those works, we study a more complex problem of scene depth estimation: the difficulties lie in per-pixel and continuous range values as outputs, in contrast to global and discrete outputs for image classification. Even for the same environments, images and depth captures can vary greatly, such as adjacent frames for a close-view object can be large room spaces. This observation indicates that our tasks are without clear task boundaries under meta-learning’s context [31], and thus we propose to treat each training sample as a **fine-grained task**.

We follow the gradient-based meta-learning, which adopts a meta-optimizer and a base-optimizer [21, 54]. The base-optimizer explores multiple inner steps to find weight-updating directions. Then the meta-optimizer updates the meta-parameters following the explored trends. After few epochs of bilevel training, we learn a mapping function θ^{prior} from image to depth. It becomes better initialization for the subsequent supervised learning (Fig. 2). We explain the improvements lie in progressive learning style. Note that meta-learning and the following supervised learning operate on the same training set without using extra data.

Previous study [89] points out indoor depth is especially hard to robustly resolve from 2D due to *complex object arrangements in near fields and arbitrary camera poses* that capture scenes from wide ranges of viewpoints. It contrasts driving scenes [18, 76, 78, 79], where decent scene a priori is given by that sky and roads dominate the upper and lower parts, and the yaw angle takes up an anchored camera rotation. Furthermore, in addition to complex scene composition and object arrangement in the near fields, surface textures or decorations can cause confusion. A depth estimator needs to separate *depth-relevant/irrelevant low-level cues*. The former indicates depth changes along with color and appearance, such as boundaries between objects and background; the latter is surface textures where depth is invariant to colors such as material patterns of walls or paintings [14, 87, 89].

We show that meta-learning induces a prior with **higher generalizability to unseen scenes with better image-to-depth understanding**, which can identify depth-relevant/irrelevant cues more robustly and suppress depth-irrelevant cues. To validate the generalizability brought by meta-learning, we adopt multiple popular indoor datasets [59, 63, 70, 89] and devise protocols for **zero-shot cross-dataset evaluation**. This greatly differs from most previous works focusing only on intra-dataset evaluation, training and testing on a single dataset, which does not validate in-the-wild

performances for practical use, such as applying to user-collected data by different cameras. We qualitatively and quantitatively show consistently superior performance by meta-learning on various network structures, including general and dedicated depth estimation architecture. The work not only focuses on improvements in depth estimation. From meta-learning’s perspective, we introduce fine-grained task on a continuous, per-pixel, and real-valued regression problem to advance meta-learning’s study on practical problems.

Contributions:

- The first method to apply meta-learning on pure single image depth prediction to achieve more generalizable and higher-performing image-to-depth understanding without using additional training data, side information, or pre-trained networks.
- A novel fine-grained task concept in meta-learning to overcome the challenging single-image setting without obvious task boundaries. This becomes an empirical study for a complicated and practical target in meta-learning.
- A devised protocol for zero-shot cross-dataset evaluation of indoor scenes to faithfully evaluate a model’s robustness and generalizability. Extensive experiments validate effectiveness of our meta-initialization strategy to learn a better image-to-depth prior.

2. Related Work

2.1. Depth from Single Indoor Images

Estimating depth from single images for indoor scenes [11, 33, 37–39, 44, 46, 60, 83, 95, 100, 101] has gained higher popularity with more high-quality datasets become available, such as Hypersim [63], Replica [70], HM3D [59], and VA [89] for photorealistic renderings from 3D environments. In addition to fundamental pixel-wise regression loss in supervised learning, some methods adopt normal [5, 93], plane constraints [38, 42, 44, 55, 95], advanced loss functions [8, 24, 48], auxiliary depth completion [28], mixed-dataset training [10, 61, 62, 94], or module customized for depth estimation [9, 40, 46, 47, 96]. In contrast, our work focuses on designing a better learning scheme: using meta-learning to improve generalizability for better image-to-depth understanding with the simplest L_2 regression loss and off-the-shelf architecture, which makes our analysis clear and without loss of generalization in methodology.

Most indoor-focused works are limited in intra-dataset evaluation, mainly on NYUv2 [69] with outdated camera models and almost frontal camera pose that cannot verify a model’s robustness for practical use. We instead devise zero-shot cross-dataset evaluation protocols using several recent high-quality synthetic and real datasets.

2.2. Gradient-based Meta-Learning

Meta-Learning principles [32, 66, 82] illustrate an oracle for learning how to learn, especially for domain adaption,

Prior learning stage

Inside each meta iteration:

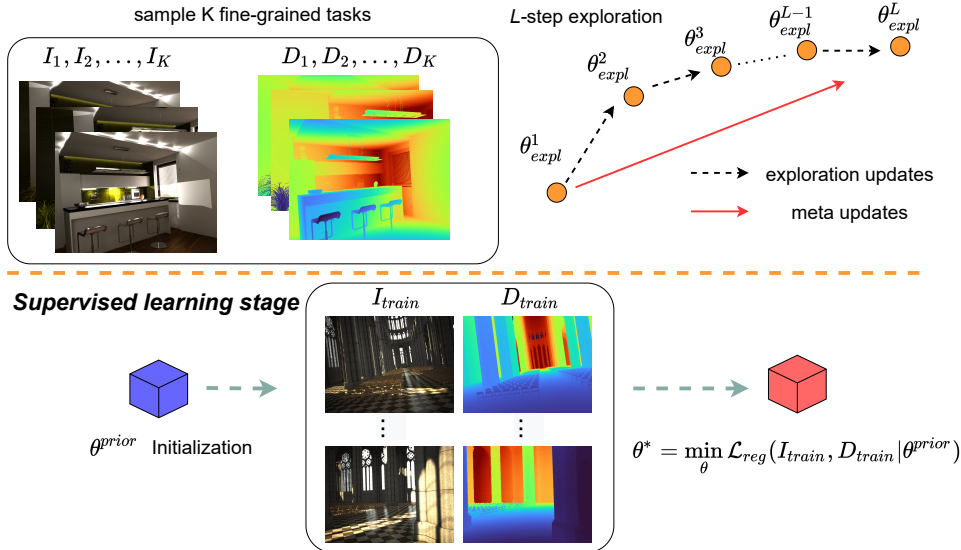


Figure 2. **Meta-Initialization for learning image-to-depth mappings.** The prior learning stage adopts a base-optimizer and a meta-optimizer. Inside each meta-iteration, K fine-grained tasks are sampled and used to minimize regression loss. L steps are taken by the base-optimizer to search for weight update directions for these K tasks. Then, the meta-optimizer follows the explored inner trends to update meta-parameters in the Reptile style [54]. Image-to-depth prior θ^{prior} is output at the end of the stage. θ^{prior} is then used as the initialization for the subsequent supervised learning for the final model θ^* .

generalization, and few-shot learning purposes. Popular gradient-based algorithms such as MAML [21] and Reptile [54] are formulated as bilevel optimization with a base- and meta-optimizer. MAML uses gradients computed on the query set to update the meta-parameters. Reptile does not distinguish support and query set and simply samples data from task distribution and updates meta-parameters by differences between inner and meta-parameters. We refer readers to [34] for algorithm survey [2, 3, 16, 21, 53, 54, 57, 58, 91, 92].

The majority of meta-learning for vision focuses on image classification [6, 7, 12, 15, 19, 36, 41, 45, 56, 68, 86, 91, 99] or pixel-level classification [1, 13, 27, 29, 43, 51, 74]. [25] pioneers to study on image regression. Still, their studied problem is considered simple that regresses a rotation angle for single synthetic object. Objects are usually overlaid on all-white or out-of-context images which are far from real.

Some works use meta-learning for depth but only for driving scenes with very different problem setup. [75, 97, 98] are built under online learning and adaptation using stereo or monocular videos for temporal consistency. They require affinity in nearby frames and meta-optimize within a single sequence, while our method is non-online, purely for single images, and meta-optimizes across multiple environments in a training set without temporal/ stereo frames. [71] groups several driving datasets as tasks but requires multiple training sets. We are the first to study meta-learning for depth from single images without assuming nearby frame affinity. The problem is arguably harder due to high appearance variation

for single images from various environments. We propose fine-grained task to fulfill learning from pure single images.

3. Methods

3.1. Difficulty in Accurate Depth Estimation

A model needs to distinguish *depth-relevant* and *depth-irrelevant low-level cues* to accurately estimate depth from images. The former shows color or radiance changes at object boundaries to the background. In the latter case, geometry is invariant to color changes, such as decoration or object textures (see Supp Sec. C). Depth-irrelevant cues frequently appear in indoor scenes due to cluttered textured objects in near fields. For example, a painting triggers many depth-irrelevant features and confuses networks. It then heavily relies on sufficient variety in training data, which demonstrate mappings from images to depth and enable learning from global context to suppress such local high-frequency details. For example, [10, 61, 62] train on mixed data sources to robustly estimate depth in the wild. When training set size is limited, there are no sufficient examples to describe mappings between the two domains. A model can either not be able to estimate precise depth or simply memorize seen image-depth pairs but cannot generalize to unseen examples [4, 20]. See Fig. 5. Thus, we exploit meta-learning with its advantages that without extra data sources, it attains few-shot learning and higher generalizability. To adapt meta-learning to single-image depth estimation, we

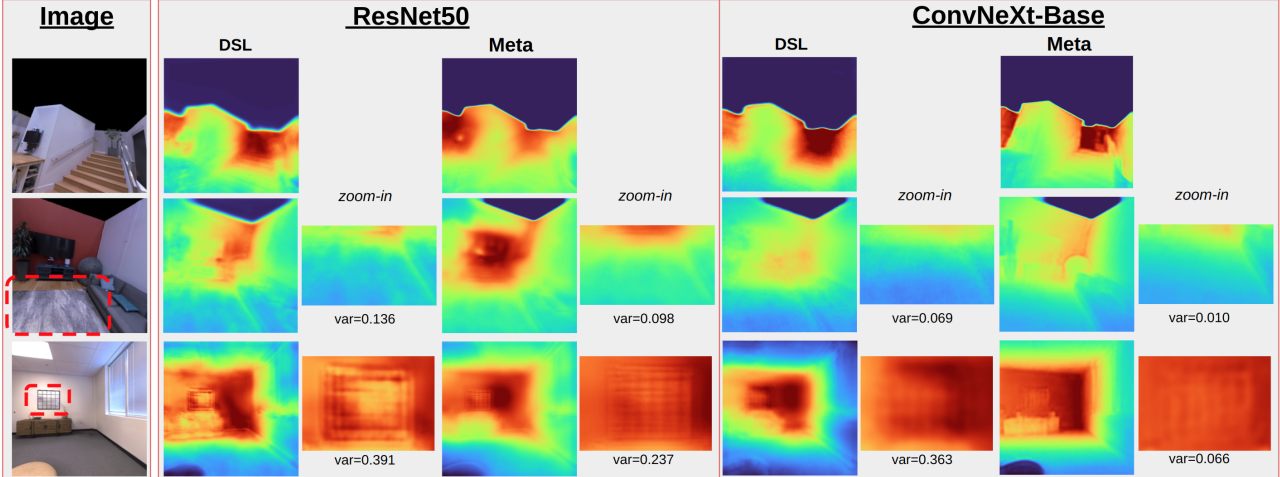


Figure 3. **Fitting to training environments.** *var* shows depth variance in the highlighted regions. We show comparison of fitting to training environments between pure meta-learning (Meta) and direct supervised learning (DSL) on limited scene-variety dataset, Replica. Meta produces smooth and more precise depth. Depth-irrelevant textures on planar regions can be resolved more correctly. In contrast, DSL produces irregularities affected by local high-frequency details, especially ResNet50. See Sec. 4.1 for details and 3.4 for the explanation.

propose fine-grained task as follows.

3.2. Single RGB-D Pair as Fine-Grained Task

Definition. Single-image depth prediction learns a function $f_\theta : \mathcal{I} \rightarrow \mathcal{D}$, parameterized by θ , to map from imagery to depth. A training set $(\mathbb{I}_{train}, \mathbb{D}_{train})$, containing image $I \in \mathbb{I}_{train}$ and associated depth map $D \in \mathbb{D}_{train}$, is used to train a model. In a minibatch with size K , each pair (I_i, D_i) , $\forall i \in [1, K]$ is treated as a **fine-grained task**. Fine-grained tasks are mutual-exclusive: no two scenes sampled from the meta-distribution, i.e., the whole RGB-D dataset, share the same scene appearance and depth relation. Proof: assume we have two different scene images I_1 and I_2 , and each contains sets of regions \mathbb{R}_1 and \mathbb{R}_2 . The null set $\phi \notin \mathbb{R}^-$, where $\mathbb{R}^- = (\mathbb{R}_1 - \mathbb{R}_2) \cup (\mathbb{R}_2 - \mathbb{R}_1)$ that contains regions appear only in either I_1 or I_2 , since I_1 and I_2 are different frames and inevitably capture different regions. Thus, any two scenes have different appearance and depth relations.

Difference with task in meta-learning. Fine-grained tasks are different from tasks in most-used meta-learning or few-shot learning usages [21], where a task contains data distribution and batches are sampled from it. Fine-grained tasks do not contain data distribution but are sampled from meta-distribution, the whole RGB-D dataset. For example, a navigating agent captures image and depth pairs. The RGB-D pairs are sampled from the meta-distribution.

Design. Each fine-grained task is used to learn on the specific RGB-D pair. The design is motivated by the fact that appearance and depth variation can be high. A view looking at small desk objects and a view of large room spaces are highly dissimilar in contents and ranges. Mappings from their scene appearance to range values are different. Still, they can be captured in the same environment or even in neighboring frames. This contrasts with image classification

where class samples share a common label. The observation explains why we treat each RGB-D pair as a fine-grained task instead of each environment.

3.3. Meta-Initialization on Depth from Single Image

We describe our approach based on gradient-based meta-learning to learn a good initialization (Fig. 2).

Prior learning stage. In the first prior learning stage, we adopt a meta-optimizer and a base-optimizer. In each meta-iteration, K fine-grained tasks as a minibatch are sampled from the whole training set: $(I_i, D_i) \sim (\mathbb{I}_{train}, \mathbb{D}_{train})$, $\forall i \in [1, K]$. Then we take L steps to explore gradient directions that minimize the regression loss and get $(\theta_{expl}^1, \theta_{expl}^2, \dots, \theta_{expl}^L)$:

$$\theta_{expl}^i \leftarrow \theta_{expl}^{i-1} - \alpha \frac{1}{K} \nabla_\theta \sum_{k \in [1, K]} \mathcal{L}_{reg}(I_k, D_k; \theta_{expl}^{i-1}), \forall i \in [1, L]. \quad (1)$$

After the L -step exploration, we update the meta-parameters using Reptile style [54], i.e., following the explored weight updating direction in the inner steps.

$$\theta_{meta}^j \leftarrow \theta_{meta}^{j-1} - \beta (\theta_{meta}^{j-1} - \theta_{expl}^L), \quad (2)$$

where α and β are respective learning rates. i and j denote inner and meta-iterations.

Compared with MAML [21], we find Reptile is more suitable for training for fine-grained tasks. First, as mentioned in Reptile’s paper [54], it is designed without support and query set split, and thus it inherently does not require multiple data samples in a task, which matches our fine-grained task definition. Next, first-order MAML computes gradients on the query set at the last inner step θ_{expl}^L to update meta-parameters. However, only one sample exists in each fine-grained task, and each fine-grained task is mutual-exclusive and can differ greatly, depending on \mathbb{R}^- . Thus, if

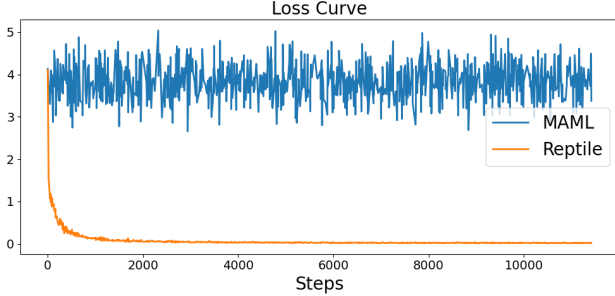


Figure 4. Loss curve for MAML v.s. Reptile.

taking exploration on a support split and computing gradients on the query split, but the support and query samples do not share common components, the gradients are nearly random and prevent from converging. By contrast, Reptile does not entail support and query split or require common components between samples, so it stabilizes training towards convergence and becomes the choice. We show the loss curve in Fig. 4.

Supervised learning stage. Prior knowledge θ^{prior} is learned after the first stage. We treat it as the initialization for the subsequent supervised learning with conventional stochastic gradient descent to minimize the regression loss.

$$\theta^* \leftarrow \min_{\theta} \mathcal{L}_{reg}(\mathbb{I}_{train}, \mathbb{D}_{train} | \theta^{prior}). \quad (3)$$

Last, the test set $(\mathbb{I}_{test}, \mathbb{D}_{test})$ is used to evaluate the depth estimation performance of θ^* . Algorithm 1 organizes the whole procedure, and we show the pseudo-code in Supp Sec. G. The implementation only needs a few-line codes as plugins to depth estimation frameworks, which benefits higher model generalizability as shown in later experiments.

Difference with other learning strategies. Compared with widely-used pretraining that requires multiple data sources to gain generalizability [61, 62, 94], both the prior learning and supervised learning stages operate on the same dataset without access to extra data or off-the-shelf models. Thus, they are free from those burdens.

Compared with simple gradient accumulation [65], where gradients are accumulated for several batches and then used to update parameters only once, the bilevel optimization keeps updating the inner-parameters every step in L to find the local niche for the current batch. Besides, gradient accumulation has the effect of large batch size, which might cause overfitting and degrade model generalizability.

3.4. Strategy and Explanation

Meta-Initialization. We next analyze meta-learning behavior with fine-grained task. Inside each meta-iteration, the base-learner explores the neighborhood with L -step using K fine-grained tasks. Compared with simple single-step update, the meta-update can be seen as first taking L -step amortized gradient descent with a lower learning rate to delicately explore local loss manifolds, then updating meta-parameters by

Algorithm 1 Our Meta-Initialization Procedure

```

1: for epoch = 1 :  $N$  do
2:   for  $j = 1 : T$  (iterations) do
3:      $\theta_{expl}^0 \leftarrow \theta_{meta}^j; (I_1, D_1), (I_2, D_2) \dots (I_K, D_K) \sim$ 
        $(\mathbb{I}_{train}, \mathbb{D}_{train})$ .
4:     for  $i = 1 : L$  (steps) do
5:        $\theta_{expl}^i \leftarrow \theta_{expl}^{i-1} - \alpha \frac{1}{K} \nabla_{\theta} \sum_{k \in [1, K]} \mathcal{L}_{reg}(I_k, D_k; \theta_{expl}^{i-1})$ .
6:     end for
7:      $\theta_{meta}^j \leftarrow \theta_{meta}^{j-1} - \beta(\theta_{meta}^{j-1} - \theta_{expl}^L)$ .
8:   end for
9: end for
10: Prior  $\theta^{prior} \leftarrow \theta_{meta}^T$  at epoch  $N$ .
11: Use  $\theta^{prior}$  as initialization. Supervised learning by
     $\theta^* \leftarrow \min_{\theta} \mathcal{L}_{reg}(\mathbb{I}_{train}, \mathbb{D}_{train} | \theta^{prior})$ .

```

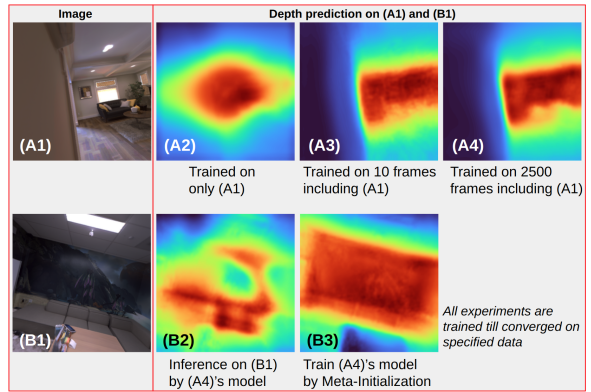


Figure 5. Analysis on scene variety and model generalizability. (A) shows limited training scenes constrain learning image-to-depth mappings, with an extreme case (A2) for only one training image. (B) shows though a model (A4) fits well on training scenes, it still cannot generalize to unseen seen, especially wall paintings with many depth-irrelevant cues. Meta-initialization attains better model generalizability. See Sec. 3.4 for explanation.

trends shown in the inner steps with a step size β towards θ^L . θ^{prior} after the prior learning may underfit the training set since the algorithm suggests not wholly following optimal gradients for each batch but with a β for control. However, it avoids overfitting to seen RGB-D pairs and forces the inner exploration to reach higher-level image-to-depth understanding. θ^{prior} then becomes good initialization for downstream RGB-D learning.

Progressive learning perspective. Algorithm 1 can be seen as progressive learning on a training set. At the first stage, meta-learning benefits learning coarse but smooth depth from global context. In Fig. 3 we apply the first-stage meta-learning compared to direct supervised learning on a dataset of limited scene variety. Meta-learning estimates smooth depth shapes and is free from irregularity that direct supervised learning encounters. The irregularity indicates the dataset did not provide sufficient scene variety that demonstrates how images map to depth in various environments to learn smooth depth from global context.

Consequently, only local high-frequency cues show. To illustrate, if only sparse and irrelevant scene images are presented, finding a function that satisfactorily fits those scenes with smooth depth from global context is hard. See Fig. 5. The irregularity occurs especially at cluttered objects or surface textured areas, since those *depth-irrelevant local cues are barely suppressed*. In summary, the progressive fashion first learns coarse but smooth depth by θ^{prior} . Then, the network learns finer depth at the second supervised stage.

4. Experiments and Discussion

Aims. We validate our meta-initialization with five questions. **Q1** Can meta-learning improve learning image-to-depth mapping on limited scene-variety datasets? (Sec. 4.1) **Q2** What improvements can meta-initialization bring compared with the most popular ImageNet-initialization? (Sec. 4.2) **Q3** How does meta-initialization help zero-shot cross-dataset generalization? (Sec. 4.3) **Q4** How does more accurate depth help learn better 3D representation? (Sec. 4.4) **Q5** How is the proposed fine-grained task related to other meta-learning findings? (Supp Sec. D)

Datasets: Exemplar data are illustrated in Supp Sec. B.

- Hypersim [63] has high scene variety with 470 synthetic indoor environments, from small rooms to large open spaces, with about 67K training and 7.7K testing images.
- HM3D [59] and Replica [70] are associated with 200K and 40K images that are taken from SimSIN [89]. HM3D has 800 scenes with *much higher scene variety* than Replica, which only has 18 overlapping scenes.
- NYUv2 [69] contains real 654 testing images. It uses older camera models with high imaging noise and limited camera viewing direction.
- VA [89] consists of 3.5K photorealistic renderings for testing on challenging lighting conditions and arbitrary camera viewing directions.

Training Settings. We use ResNet [30], ConvNeXt [49], and their variants as the network architecture to extract bottleneck features. Then we build a depth regression head following [26] containing 5 convolution blocks with skip connection from the encoder. Each convolution block contains a 3x3 convolution, an ELU activation, and a bilinear $2\times$ upsampling layer to recover the input size at the end output. Channel-size of each convolution block is (256, 128, 64, 32, 16). Last, a 3x3 convolution for 1-channel output with a sigmoid activation are used to get inverse depth, which is then converted to depth [18]. We set $N = 5$, $L = 4$, $K = 50$, $(\alpha, \beta) = (0.001, 0.5)$ for ResNet, and $(\alpha, \beta) = (0.0005, 0.5)$ for ConvNeXt. At the supervised learning stage, we train models for 15 epochs with a learning rate of 3×10^{-4} , optimized by AdamW [50] with a weight decay of 0.01. Input size to the network is 256×256 . L_2 loss is used as \mathcal{L}_{reg} .

Metrics. We adopt common monocular depth estimation evaluation metrics. Error metrics (in meters, the lower the better): Mean Absolute Error (MAE), Absolute Relative Error (AbsRel), Root Mean Square Error (RMSE). Threshold Accuracy: δ_C (in %, percentage of correct pixel depth. Higher percentage implies more structured depth hence better). Correctness: ratio between prediction and groundtruth is within 1.25^C , $C = [1, 2, 3]$.

4.1. Meta-Learning on Limited Scene Variety

We first show how a single-stage meta-learning (only prior stage) performs. We train $N=15$ epochs of meta-learning and compare with 15 epochs of direct supervised learning where both training pieces converge already. The other hyperparameters are the same as given in Training Settings. Replica Dataset of limited scene variety is used to verify gain on limited sources. Fig. 3 show fitting to training scenes. From the figure, meta-learning is capable of identifying near and far fields without irregularity that direct supervised learning struggles with. Under limited training scenes, meta-learning induces a better image-to-depth mapping that delineates object shapes, separates depth-relevant/-irrelevant cues, and shows flat planes where rich depth-irrelevant textures exist. The observation follows the explanation in Sec. 3.4. See Supp Sec. C for more analysis.

We next numerically examine generalizability to unseen scenes when training on different level scene-variety data. HM3D (high scene variety) and Replica (low scene variety) are used as training sets and VA is used for testing. Table 1 shows that models trained by single-stage meta-learning substantially outperform direct supervised learning with 15.7%-29.4% improvements. The advantage is more evident when trained on lower scene-variety Replica.

4.2. Meta-Initialization v.s. ImageNet-Initialization

Sec. 4.1 shows single-stage meta-learning induces much better depth regression, but the depth is yet detailed. We next train full Algorithm 1, using meta-learned weights as initialization for following supervised learning. We **go beyond limited sources** and train on higher scene-variety datasets. Intuitively, higher scene variety helps supervised learning attain better depth prediction and might diminish meta-learning’s advantages of few-shot and low-source learning. However, such studies are practical for validating meta-learning in real-world applications. Comparison is drawn with baselines of direct supervised learning without meta-initialization that begins from ImageNet-initialization instead.

Table 2 shows intra-dataset evaluation that trains/ tests on each official data splits. For Hypersim evaluation is capped for depth at 20m and 10m for NYUv2. Uniquely, using meta-initialization attains **consistently** lower errors and higher accuracy than the baselines, especially AbsRel (averagely +6.5%) and δ_1 (averagely +1.69 points) that in-

Table 1. **Generalizability with different scene variety.** We compare single-stage meta-learning (only prior learning) and supervised learning. ConvNeXt-Base backbone is used. $a \rightarrow b$ means training on a - and testing on b -dataset. Replica and HM3D respectively hold lower and higher scene variety for training. Meta-Learning has much larger improvements especially trained on low scene-variety Replica.

Method	Replica \rightarrow VA			HM3D \rightarrow VA		
	MAE	AbsRel	RMSE	MAE	AbsRel	RMSE
Direct supervised learning	0.718	0.538	1.078	0.544	0.456	0.715
Meta-Learning	0.548	0.430	0.761	0.427	0.369	0.603
Improvement	-23.6%	-20.1%	-29.4%	-21.5%	-19.1%	-15.7%

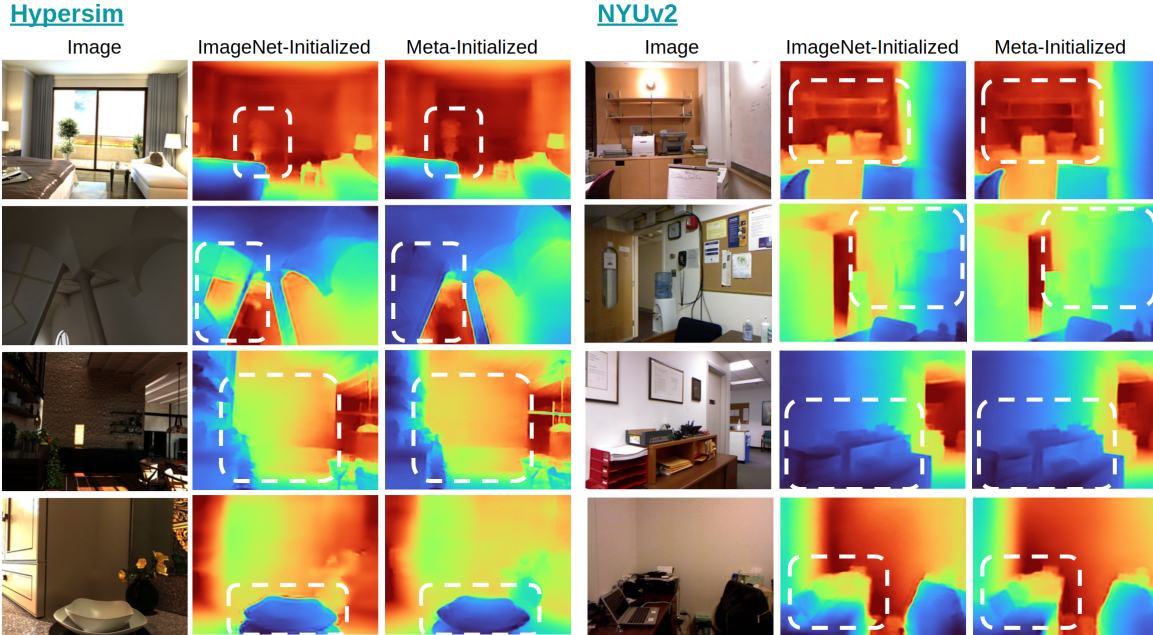


Figure 6. **Depth map qualitative comparison.** Results of our meta-initialization have better object shapes with clearer boundaries. Depth-irrelevant textures are suppressed, and flat planes are predicted, as shown in Hypersim- Row 2 ceiling and 3 textured wall examples.

Table 2. **Effects of Meta-Initialization on intra-dataset evaluation.** We train and test meta-initialization (full Algorithm 1) on the same dataset. Hypersim and NYUv2 of higher scene variety are used. Using the same architecture, meta-initialization (+Meta) consistently outperforms ImageNet-initialization (no marks). Both error (in orange) and accuracy (in green) are reported.

Hypersim	MAE	AbsRel	RMSE	δ_1	δ_2	δ_3
ResNet50	1.288	0.248	1.775	64.8	87.1	94.7
ResNet50 + Meta	1.205	0.239	1.680	66.7	87.9	95.0
ResNet101	1.197	0.234	1.671	67.4	88.5	95.3
ResNet101 + Meta	1.158	0.220	1.595	68.0	89.0	95.4
ConvNeXt-base	1.073	0.201	1.534	73.6	91.1	96.3
ConvNeXt-base + Meta	0.994	0.188	1.425	74.9	91.7	96.5
NYUv2	MAE	AbsRel	RMSE	δ_1	δ_2	δ_3
ResNet50	0.345	0.131	0.480	83.6	96.4	99.0
ResNet50 + Meta	0.325	0.122	0.454	85.4	96.8	99.3
ResNet101	0.318	0.120	0.448	85.6	97.1	99.3
ResNet101 + Meta	0.303	0.112	0.420	86.7	97.4	99.4
ConvNeXt-base	0.273	0.101	0.394	89.4	97.9	99.5
ConvNeXt-base+Meta	0.266	0.099	0.387	89.8	98.1	99.5

indicates accurate depth structure is predicted. We further display qualitative comparison for depth and 3D point cloud view in Fig. 6 and 1. The gain simply comes from better training schema without more data or constraints, advanced loss, or model design. More results are in Supp Sec. G.

4.3. Zero-Shot Cross-Dataset Evaluation

To faithfully validate a trained model in the wild, we design protocols for zero-shot cross-dataset inference. High scene-variety and larger-size synthetic datasets, Hypersim and HM3D, are used as training sets. VA, Replica, and NYUv2 serve as testing, and their evaluations are capped at 10m. We median-scale prediction to groundtruth in the protocol to compensate for different camera intrinsic. In Table 3, compared with ImageNet-initialization, meta-initialization **consistently** improves in nearly all the metrics, especially δ_1 (averagely +1.97 points). The gain comes from that meta-prior attains a better image-to-depth mapping with coarse but smooth and reasonable depth. Conditioned on the initialization, the learning better calibrates to open-world image-to-depth relation hence generalizes better to unseen scenes.

We further experiment on recent high-performing architecture dedicated to depth estimation, including BTS [42], DPT (hybrid and large size) [61], and DepthFormer [46]. Table 4 displays the comparison and shows that meta-initialization consistently improves performance for zero-shot cross-dataset inference using the dedicated architectures, gearing higher generalizability for the existing models.

Table 3. **Zero-Shot cross-dataset evaluation using meta-initialization (Algorithm 1)**. Comparison is drawn between without meta-initialization (no marks, ImageNet-initialization) and with our meta-initialization (Meta) using different sizes ConvNeXt. Results of "+Meta" are consistently better.

HM3D → VA	MAE	AbsRel	RMSE	δ_1	δ_2	δ_3
ConvNeXt-small	0.267	0.180	0.389	74.6	91.0	96.1
ConvNeXt-small + Meta	0.233	0.162	0.345	77.8	93.1	97.3
ConvNeXt-base	0.258	0.176	0.385	76.1	91.1	95.4
ConvNeXt-base + Meta	0.238	0.163	0.356	78.0	92.5	96.7
ConvNeXt-large	0.242	0.170	0.357	78.1	91.5	95.7
ConvNeXt-large + Meta	0.226	0.160	0.330	78.9	92.2	96.3
HM3D → NYUv2	MAE	AbsRel	RMSE	δ_1	δ_2	δ_3
ConvNeXt-small	0.540	0.213	0.728	69.2	88.7	95.8
ConvNeXt-small + Meta	0.527	0.206	0.710	70.7	89.0	95.9
ConvNeXt-base	0.529	0.208	0.717	70.1	89.4	96.0
ConvNeXt-base + Meta	0.505	0.199	0.691	71.6	89.8	96.3
ConvNeXt-large	0.501	0.192	0.690	72.0	90.4	96.4
ConvNeXt-large + Meta	0.481	0.190	0.660	73.2	90.6	96.6
HM3D → Replica	MAE	AbsRel	RMSE	δ_1	δ_2	δ_3
ConvNeXt-small	0.222	0.138	0.321	84.5	93.9	96.6
ConvNeXt-small + Meta	0.200	0.126	0.287	85.6	95.7	98.1
ConvNeXt-base	0.217	0.134	0.316	84.6	94.2	96.6
ConvNeXt-base + Meta	0.192	0.117	0.277	87.1	96.4	98.5
ConvNeXt-large	0.214	0.137	0.307	84.3	94.0	96.6
ConvNeXt-large + Meta	0.191	0.117	0.275	87.1	96.5	98.5
Hypersim → VA	MAE	AbsRel	RMSE	δ_1	δ_2	δ_3
ConvNeXt-small	0.291	0.215	0.404	68.5	90.8	96.7
ConvNeXt-small + Meta	0.280	0.207	0.398	70.4	91.3	97.0
ConvNeXt-base	0.275	0.201	0.393	71.3	91.8	97.3
ConvNeXt-base + Meta	0.259	0.194	0.365	72.8	92.8	97.8
ConvNeXt-large	0.263	0.198	0.369	73.0	92.0	97.1
ConvNeXt-large + Meta	0.248	0.183	0.355	74.6	93.5	97.8
Hypersim → NYUv2	MAE	AbsRel	RMSE	δ_1	δ_2	δ_3
ConvNeXt-small	0.434	0.165	0.598	75.7	94.3	98.5
ConvNeXt-small + Meta	0.415	0.155	0.575	77.8	95.1	98.8
ConvNeXt-base	0.396	0.150	0.549	79.6	95.6	98.9
ConvNeXt-base + Meta	0.386	0.141	0.524	80.3	96.0	99.0
ConvNeXt-large	0.389	0.149	0.542	79.8	95.6	98.8
ConvNeXt-large + Meta	0.375	0.140	0.517	81.2	96.2	99.1
Hypersim → Replica	MAE	AbsRel	RMSE	δ_1	δ_2	δ_3
ConvNeXt-small	0.307	0.189	0.417	72.4	92.1	97.5
ConvNeXt-small + Meta	0.294	0.178	0.404	74.5	92.7	97.5
ConvNeXt-base	0.312	0.185	0.429	74.1	92.6	97.4
ConvNeXt-base + Meta	0.288	0.173	0.399	75.6	93.3	97.9
ConvNeXt-large	0.285	0.172	0.394	75.8	93.2	97.7
ConvNeXt-large + Meta	0.273	0.165	0.380	77.0	94.0	98.1

4.4. Depth Supervision in NeRF

We show that more accurate depth from meta-initialization can better supervise the distance d a ray travels in NeRF. d is determined by the volumetric rendering rule [17]. Additional to pixel color loss, we use monocular predicted distance map d^* , converted from depth, to supervise the training by $\mathcal{L}_D = |d^* - d|$. The experiment is conducted on Replica’s office-0 environment with 180 training views. After 30K training steps, we obtain NeRF-rendered views and calculate commonly-used image quality metrics (PSNR and SSIM, the higher the better). We use ConvNeXt-base to predict d^* . The comparison is made between using (A) without meta-initialization and (B)

Table 4. **Cross-Dataset evaluation using dedicated depth estimation networks**. Our meta-initialization (+Meta) can be plugged into several methods to stably improve them.

Hypersim → Replica	MAE	AbsRel	RMSE	δ_1	δ_2	δ_3
BTS-ResNet50 [42]	0.365	0.226	0.505	69.5	88.9	96.2
BTS-ResNet50 + Meta	0.328	0.208	0.475	70.6	90.0	96.5
BTS-ResNet101 [42]	0.339	0.214	0.488	69.9	89.8	96.3
BTS-ResNet101 + Meta	0.322	0.200	0.469	71.0	90.4	96.8
DepthFormer [46]	0.303	0.185	0.415	72.9	92.3	97.4
DepthFormer + Meta	0.292	0.180	0.400	74.3	92.7	97.5
DPT-hybrid [61]	0.315	0.197	0.455	71.2	90.7	96.7
DPT-hybrid + Meta	0.289	0.170	0.396	75.6	93.5	97.8
DPT-large [61]	0.294	0.172	0.401	75.4	93.3	97.6
DPT-large + Meta	0.268	0.162	0.376	77.2	94.2	98.1
AdaBins [8]	0.331	0.210	0.445	70.2	90.1	96.6
AdaBins + Meta	0.319	0.198	0.432	71.7	92.0	97.3
GLPDepth [40]	0.309	0.188	0.418	72.9	92.4	97.6
GLPDepth + Meta	0.290	0.175	0.400	74.6	92.8	97.7
Hypersim → NYUv2	MAE	AbsRel	RMSE	δ_1	δ_2	δ_3
BTS-ResNet50 [42]	0.487	0.196	0.654	71.8	90.4	95.6
BTS-ResNet50+Meta	0.455	0.178	0.628	73.9	92.4	97.3
BTS-ResNet101 [42]	0.468	0.187	0.641	72.3	90.8	95.8
BTS-ResNet101+Meta	0.450	0.175	0.623	74.2	92.6	97.5
DepthFormer [46]	0.442	0.169	0.608	75.1	93.9	98.2
DepthFormer + Meta	0.416	0.157	0.580	77.8	94.3	98.2
DPT-hybrid [61]	0.409	0.149	0.580	78.9	94.8	98.3
DPT-hybrid + Meta	0.395	0.140	0.559	81.0	96.4	99.1
DPT-large [61]	0.373	0.136	0.534	82.3	96.2	98.8
DPT-large + Meta	0.364	0.131	0.520	83.2	96.6	99.1
AdaBins [8]	0.469	0.188	0.642	72.6	91.2	96.6
AdaBins+Meta	0.448	0.175	0.625	74.0	92.6	97.4
GLPDepth [40]	0.438	0.169	0.604	75.3	93.9	98.2
GLPDepth+Meta	0.414	0.158	0.583	77.9	94.3	98.3

with meta-initialization. Results: (A): (38.67, 0.9629), (B): (39.29, 0.9680). The results show better image quality is attained induced by better 3D representation in depth from meta-initialization. See more results in Supp Sec. F.

5. Conclusion and Limitation

We first validate single-stage meta-learning estimates coarse but smooth depth from global context (4.1). It is a better initialization for the following supervised learning to obtain higher model generalizability on intra-dataset and zero-shot cross-dataset evaluation (4.2, 4.3), as well as a better 3D representation in NeRF training. (4.4).

From depth’s perspective,

- this work provides a simple learning scheme to gain generalizability without needs of extra data, constraints, advanced loss, or module design;
- is easy to plug into general architecture or dedicated depth framework and show concrete improvements;
- proposes zero-shot cross-dataset protocol to attend to in-the-wild performance that most prior work overlook.

From meta-learning’s perspective,

- this work chooses the challenging single-image setting and meta-optimizes across environments, unlike prior works for online video adaptation that meta-optimizes within a sequence with access to multiple frames;

- proposes fine-grained task to overcome lacks of affinity in sparse and irrelevant sampled images.
- studies a complex single-image real-valued regression problem rather than widely-studied classification.

The work is at intersection of the two research fields and we hope it drives the dual-stream research development.

Discussion: large foundation models. Those models require a large corpus of pretrained data and still need a finetune RGB-D dataset to adapt, and we only require an RGB-D set. If the size of finetune set is not large, a large model may easily overfit by overparameterization and show lower generalization. We experiment finetuning foundation models using ConvNeXt-XXLarge and ViT-L/14 and compare with our meta-initialization. They are CLIP weights first and further tuned on ImageNet22K. Finetuning foundation models does not win over our +Meta on Replica \rightarrow VA and only show marginal gain on HM3D \rightarrow VA.

AbsRel \downarrow	ConvNeXt-XXLarge	ViT-L/14	ConvNeXt-Base+Meta
Replica \rightarrow VA	0.437	0.434	0.430
HM3D \rightarrow VA	0.160	0.162	0.163

Limitation This work focuses on estimating depth from single images, which has wide applications in 3D-aware image synthesis or inpainting when an online depth estimator is needed. Other scopes of depth from images, such as stereo, multiview, video, or online learning is beyond our scope.

References

- [1] Mustafa Sercan Amac, Ahmet Sencan, Bugra Baran, Nazli Ikizler-Cinbis, and Ramazan Gokberk Cinbis. Masksplit: Self-supervised meta-learning for few-shot semantic segmentation. In *WACV*, 2022. 3
- [2] Marcin Andrychowicz, Misha Denil, Sergio Gomez, Matthew W Hoffman, David Pfau, Tom Schaul, Brendan Shillingford, and Nando De Freitas. Learning to learn by gradient descent by gradient descent. *NeurIPS*, 2016. 3
- [3] Antreas Antoniou, Harri Edwards, and Amos Storkey. How to train your maml. In *ICLR*, 2019. 3
- [4] Devansh Arpit, Stanisław Jastrzębski, Nicolas Ballas, David Krueger, Emmanuel Bengio, Maxinder S Kanwal, Tegan Maharaj, Asja Fischer, Aaron Courville, Yoshua Bengio, et al. A closer look at memorization in deep networks. In *ICML*, 2017. 3
- [5] Gwangbin Bae, Ignas Budvytis, and Roberto Cipolla. Irondepth: Iterative refinement of single-view depth using surface normal and its uncertainty. *arXiv preprint arXiv:2210.03676*, 2022. 2
- [6] Yan Bai, Jile Jiao, Wang Ce, Jun Liu, Yihang Lou, Xuetao Feng, and Ling-Yu Duan. Person30k: A dual-meta generalization network for person re-identification. In *CVPR*, 2021. 3
- [7] Yogesh Balaji, Swami Sankaranarayanan, and Rama Chellappa. Metareg: Towards domain generalization using meta-regularization. *NeurIPS*, 2018. 3
- [8] Shariq Farooq Bhat, Ibraheem Alhashim, and Peter Wonka. Adabins: Depth estimation using adaptive bins. In *CVPR*, 2021. 2, 8
- [9] Shariq Farooq Bhat, Ibraheem Alhashim, and Peter Wonka. Localbins: Improving depth estimation by learning local distributions. In *ECCV*, 2022. 2
- [10] Shariq Farooq Bhat, Reiner Birkel, Diana Wofk, Peter Wonka, and Matthias Müller. Zoedepth: Zero-shot transfer by combining relative and metric depth, 2023. 2, 3
- [11] Jia-Wang Bian, Huangying Zhan, Naiyan Wang, Tat-Jun Chin, Chunhua Shen, and Ian Reid. Auto-rectify network for unsupervised indoor depth estimation. *TPAMI*, 2021. 2
- [12] Manh-Ha Bui, Toan Tran, Anh Tran, and Dinh Phung. Exploiting domain-specific features to enhance domain generalization. *NeurIPS*, 2021. 3
- [13] Zhiying Cao, Tengfei Zhang, Wenhui Diao, Yue Zhang, Xiaode Lyu, Kun Fu, and Xian Sun. Meta-seg: A generalized meta-learning framework for multi-class few-shot semantic segmentation. *IEEE Access*, 2019. 3
- [14] Xiaotian Chen, Yuwang Wang, Xuejin Chen, and Wenjun Zeng. S2r-depthnet: Learning a generalizable depth-specific structural representation. In *CVPR*, 2021. 2
- [15] Yinbo Chen, Zhuang Liu, Huijuan Xu, Trevor Darrell, and Xiaolong Wang. Meta-baseline: exploring simple meta-learning for few-shot learning. In *ICCV*, 2021. 3
- [16] Kurtland Chua, Qi Lei, and Jason D Lee. How fine-tuning allows for effective meta-learning. *NeurIPS*, 2021. 3
- [17] Kangle Deng, Andrew Liu, Jun-Yan Zhu, and Deva Ramanan. Depth-supervised nerf: Fewer views and faster training for free. In *CVPR*, 2022. 1, 8
- [18] Tom van Dijk and Guido de Croon. How do neural networks see depth in single images? In *ICCV*, 2019. 2, 6
- [19] Qi Dou, Daniel Coelho de Castro, Konstantinos Kamnitsas, and Ben Glocker. Domain generalization via model-agnostic learning of semantic features. *NeurIPS*, 2019. 3
- [20] Vitaly Feldman and Chiyuan Zhang. What neural networks memorize and why: Discovering the long tail via influence estimation. *NeurIPS*, 2020. 3
- [21] Chelsea Finn, Pieter Abbeel, and Sergey Levine. Model-agnostic meta-learning for fast adaptation of deep networks. In *ICML*, 2017. 2, 3, 4
- [22] Chelsea Finn, Aravind Rajeswaran, Sham Kakade, and Sergey Levine. Online meta-learning. In *ICML*, 2019. 2
- [23] Fabrizio Flacco, Torsten Kröger, Alessandro De Luca, and Oussama Khatib. A depth space approach to human-robot collision avoidance. In *ICRA*, 2012. 1
- [24] Huan Fu, Mingming Gong, Chaohui Wang, Kayhan Batmanghelich, and Dacheng Tao. Deep ordinal regression network for monocular depth estimation. In *CVPR*, 2018. 2
- [25] Ning Gao, Hanna Ziesche, Ngo Anh Vien, Michael Volpp, and Gerhard Neumann. What matters for meta-learning vision regression tasks? In *CVPR*, 2022. 3
- [26] Clement Godard, Oisín Mac Aodha, Michael Firman, and Gabriel J. Brostow. Digging into self-supervised monocular depth estimation. In *ICCV*, 2019. 6
- [27] Rui Gong, Yuhua Chen, Danda Pani Paudel, Yawei Li, Ajad Chhatkuli, Wen Li, Dengxin Dai, and Luc Van Gool. Cluster, split, fuse, and update: Meta-learning for open compound domain adaptive semantic segmentation. In *CVPR*, 2021. 3

- [28] Vitor Guizilini, Rares Ambrus, Wolfram Burgard, and Adrien Gaidon. Sparse auxiliary networks for unified monocular depth prediction and completion. In *CVPR*, 2021. 2
- [29] Xiaoqing Guo, Chen Yang, Baopu Li, and Yixuan Yuan. Metacorrection: Domain-aware meta loss correction for unsupervised domain adaptation in semantic segmentation. In *CVPR*, 2021. 3
- [30] Kaiming He, Xiangyu Zhang, Shaoqing Ren, and Jian Sun. Deep residual learning for image recognition. In *CVPR*, 2016. 6
- [31] Xu He, Jakub Sygnowski, Alexandre Galashov, Andrei A Rusu, Yee Whye Teh, and Razvan Pascanu. Task agnostic continual learning via meta learning. *arXiv preprint arXiv:1906.05201*, 2019. 2
- [32] Sepp Hochreiter, A Steven Younger, and Peter R Conwell. Learning to learn using gradient descent. In *ICANN*, 2001. 2
- [33] Aleksander Holynski and Johannes Kopf. Fast depth denoising for occlusion-aware augmented reality. In *SIGGRAPH Asia*, 2018. 2
- [34] Timothy M Hospedales, Antreas Antoniou, Paul Micaelli, and Amos J Storkey. Meta-learning in neural networks: A survey. *IEEE Transactions on Pattern Analysis and Machine Intelligence*, 2021. 2, 3
- [35] Muhammad Zubair Irshad, Chih-Yao Ma, and Zsolt Kira. Hierarchical cross-modal agent for robotics vision-and-language navigation. In *ICRA*, 2021. 1
- [36] Muhammad Abdullah Jamal and Guo-Jun Qi. Task agnostic meta-learning for few-shot learning. In *CVPR*, 2019. 3
- [37] Pan Ji, Runze Li, Bir Bhanu, and Yi Xu. Monoindoor: Towards good practice of self-supervised monocular depth estimation for indoor environments. In *ICCV*, 2021. 2
- [38] Hualie Jiang, Laiyan Ding, Junjie Hu, and Rui Huang. Plnet: Plane and line priors for unsupervised indoor depth estimation. In *3DV*, 2021. 2
- [39] Jinyoung Jun, Jae-Han Lee, Chul Lee, and Chang-Su Kim. Depth map decomposition for monocular depth estimation. 2022. 2
- [40] Doyeon Kim, Woonghyun Ga, Pyungwhan Ahn, Donggyu Joo, Sehwan Chun, and Junmo Kim. Global-local path networks for monocular depth estimation with vertical cutdepth. *arXiv preprint arXiv:2201.07436*, 2022. 2, 8
- [41] Hae Beom Lee, Taewook Nam, Eunho Yang, and Sung Ju Hwang. Meta dropout: Learning to perturb latent features for generalization. In *ICLR*, 2019. 3
- [42] Jin Han Lee, Myung-Kyu Han, Dong Wook Ko, and Il Hong Suh. From big to small: Multi-scale local planar guidance for monocular depth estimation. *arXiv preprint arXiv:1907.10326*, 2019. 2, 7, 8
- [43] Yuan-Hao Lee, Fu-En Yang, and Yu-Chiang Frank Wang. A pixel-level meta-learner for weakly supervised few-shot semantic segmentation. In *WACV*, 2022. 3
- [44] Boying Li, Yuan Huang, Zeyu Liu, Danping Zou, and Wenxian Yu. Structdepth: Leveraging the structural regularities for self-supervised indoor depth estimation. In *ICCV*, 2021. 2
- [45] Da Li, Yongxin Yang, Yi-Zhe Song, and Timothy M Hospedales. Learning to generalize: Meta-learning for domain generalization. In *AAAI*, 2018. 3
- [46] Zhenyu Li, Zehui Chen, Xianming Liu, and Junjun Jiang. Depthformer: Exploiting long-range correlation and local information for accurate monocular depth estimation. *arXiv preprint arXiv:2203.14211*, 2022. 2, 7, 8
- [47] Zhenyu Li, Xuyang Wang, Xianming Liu, and Junjun Jiang. Binsformer: Revisiting adaptive bins for monocular depth estimation. 2022. 2
- [48] Ce Liu, Suryansh Kumar, Shuhang Gu, Radu Timofte, and Luc Van Gool. Va-depthnet: A variational approach to single image depth prediction. In *ICLR*, 2023. 2
- [49] Zhuang Liu, Hanzi Mao, Chao-Yuan Wu, Christoph Feichtenhofer, Trevor Darrell, and Saining Xie. A convnet for the 2020s. *CVPR*, 2022. 6
- [50] Ilya Loshchilov and Frank Hutter. Decoupled weight decay regularization. In *ICLR*, 2018. 6
- [51] Xinyu Luo, Jiaming Zhang, Kailun Yang, Alina Roitberg, Kunyu Peng, and Rainer Stiefelwagen. Towards robust semantic segmentation of accident scenes via multi-source mixed sampling and meta-learning. In *CVPRW*, 2022. 3
- [52] Hugo Nascimento, Martin Mujica, and Mourad Benoussaad. Collision avoidance interaction between human and a hidden robot based on kinect and robot data fusion. *IEEE Robotics and Automation Letters*, 6(1):88–94, 2020. 1
- [53] Renkun Ni, Manli Shu, Hossein Souri, Micah Goldblum, and Tom Goldstein. The close relationship between contrastive learning and meta-learning. In *ICLR*, 2022. 3
- [54] Alex Nichol, Joshua Achiam, and John Schulman. On first-order meta-learning algorithms. *arXiv preprint arXiv:1803.02999*, 2018. 2, 3, 4
- [55] Vaishakh Patil, Christos Sakaridis, Alexander Liniger, and Luc Van Gool. P3Depth: Monocular depth estimation with a piecewise planarity prior. In *CVPR*, 2022. 2
- [56] Fengchun Qiao, Long Zhao, and Xi Peng. Learning to learn single domain generalization. In *CVPR*, 2020. 3
- [57] Janarthanan Rajendran, Alexander Irpan, and Eric Jang. Meta-learning requires meta-augmentation. In *NeurIPS*, 2020. 3
- [58] Aravind Rajeswaran, Chelsea Finn, Sham M Kakade, and Sergey Levine. Meta-learning with implicit gradients. *NeurIPS*, 2019. 3
- [59] Santhosh K Ramakrishnan, Aaron Gokaslan, Erik Wijmans, Oleksandr Maksymets, Alex Clegg, John Turner, Eric Undersander, Wojciech Galuba, Andrew Westbury, Angel X Chang, et al. Habitat-matterport 3D dataset (HM3D): 1000 large-scale 3D environments for embodied AI. *NeurIPS Datasets and Benchmarks Track*, 2021. 2, 6
- [60] Michael Ramamonjisoa and Vincent Lepetit. Sharpnet: Fast and accurate recovery of occluding contours in monocular depth estimation. *ICCVW*, 2019. 2
- [61] René Ranftl, Alexey Bochkovskiy, and Vladlen Koltun. Vision transformers for dense prediction. *ICCV*, 2021. 1, 2, 3, 5, 7, 8
- [62] René Ranftl, Katrin Lasinger, David Hafner, Konrad Schindler, and Vladlen Koltun. Towards robust monocular

- depth estimation: Mixing datasets for zero-shot cross-dataset transfer. *TPAMI*, 2020. 1, 2, 3, 5
- [63] Mike Roberts and Nathan Paczan. Hypersim: A photorealistic synthetic dataset for holistic indoor scene understanding. *ICCV*, 2021. 2, 6
- [64] Barbara Roessle, Jonathan T Barron, Ben Mildenhall, Pratul P Srinivasan, and Matthias Nießner. Dense depth priors for neural radiance fields from sparse input views. In *CVPR*, 2022. 1
- [65] Sebastian Ruder. An overview of gradient descent optimization algorithms. *arXiv preprint arXiv:1609.04747*, 2016. 5
- [66] Jürgen Schmidhuber. Evolutionary principles in self-referential learning, or on learning how to learn: the meta-meta-... hook. *Technische Universität München, PhD thesis*, 1987. 2
- [67] Philipp Schmidt, Nikolaus Vahrenkamp, Mirko Wächter, and Tamim Asfour. Grasping of unknown objects using deep convolutional neural networks based on depth images. In *ICRA*, 2018. 1
- [68] Yang Shu, Zhangjie Cao, Chenyu Wang, Jianmin Wang, and Mingsheng Long. Open domain generalization with domain-augmented meta-learning. In *CVPR*, 2021. 3
- [69] Nathan Silberman, Derek Hoiem, Pushmeet Kohli, and Rob Fergus. Indoor segmentation and support inference from rgb-d images. In *ECCV*, 2012. 2, 6
- [70] Julian Straub, Thomas Whelan, Lingni Ma, Yufan Chen, Erik Wijmans, Simon Green, Jakob J Engel, Raul Mur-Artal, Carl Ren, Shobhit Verma, et al. The replica dataset: A digital replica of indoor spaces. *arXiv preprint arXiv:1906.05797*, 2019. 2, 6
- [71] Qiyu Sun, Gary G Yen, Yang Tang, and Chaoqiang Zhao. Learn to adapt for monocular depth estimation. *arXiv preprint arXiv:2203.14005*, 2022. 3
- [72] Lei Tai, Jingwei Zhang, Ming Liu, and Wolfram Burgard. Socially compliant navigation through raw depth inputs with generative adversarial imitation learning. In *ICRA*, 2018. 1
- [73] Sinan Tan, Mengmeng Ge, Di Guo, Huaping Liu, and Fuchun Sun. Depth-aware vision-and-language navigation using scene query attention network. In *ICRA*, 2022. 1
- [74] Pinzhuo Tian, Zhangkai Wu, Lei Qi, Lei Wang, Yinghuan Shi, and Yang Gao. Differentiable meta-learning model for few-shot semantic segmentation. In *AAAI*, 2020. 3
- [75] Alessio Tonioni, Oscar Rahnama, Thomas Joy, Luigi Di Stefano, Thalaisyasingam Ajanthan, and Philip HS Torr. Learning to adapt for stereo. In *CVPR*, 2019. 3
- [76] Alessio Tonioni, Fabio Tosi, Matteo Poggi, Stefano Mattoccia, and Luigi Di Stefano. Real-time self-adaptive deep stereo. In *CVPR*, 2019. 2
- [77] Ulrich Viereck, Andreas Pas, Kate Saenko, and Robert Platt. Learning a visuomotor controller for real world robotic grasping using simulated depth images. In *CoRL*, 2017. 1
- [78] Jamie Watson, Michael Firman, Gabriel J Brostow, and Daniyar Turmukhambetov. Self-supervised monocular depth hints. In *ICCV*, 2019. 2
- [79] Jamie Watson, Oisín Mac Aodha, Victor Prisacariu, Gabriel Brostow, and Michael Firman. The temporal opportunist: Self-supervised multi-frame monocular depth. In *CVPR*, 2021. 2
- [80] Cho-Ying Wu and Jian-Jiun Ding. Occlusion pattern-based dictionary for robust face recognition. In *2016 IEEE International Conference on Multimedia and Expo (ICME)*, 2016. 1
- [81] Cho Ying Wu and Jian Jiun Ding. Occluded face recognition using low-rank regression with generalized gradient direction. *Pattern Recognition*, 80:256–268, 2018. 1
- [82] Cho-Ying Wu and Jian-Jiun Ding. Nonconvex approach for sparse and low-rank constrained models with dual momentum. *arXiv preprint arXiv:1906.02433*, 2019. 2
- [83] Cho-Ying Wu, Quankai Gao, Chin-Cheng Hsu, Te-Lin Wu, Jing-Wen Chen, and Ulrich Neumann. Inspace-type: Reconsider space type in indoor monocular depth estimation. *arXiv preprint arXiv:2309.13516*, 2023. 2
- [84] Cho-Ying Wu, Chin-Cheng Hsu, and Ulrich Neumann. Cross-modal perceptionist: Can face geometry be gleaned from voices? In *Proceedings of the IEEE/CVF Conference on Computer Vision and Pattern Recognition*, 2022. 1
- [85] Cho-Ying Wu, Xiaoyan Hu, Michael Happold, Qiangeng Xu, and Ulrich Neumann. Geometry-aware instance segmentation with disparity maps. *arXiv preprint arXiv:2006.07802*, 2020. 1
- [86] Cho Ying Wu and Ulrich Neumann. Efficient multi-domain dictionary learning with gans. In *2019 IEEE Global Conference on Signal and Information Processing (GlobalSIP)*, 2019. 3
- [87] Cho-Ying Wu and Ulrich Neumann. Salient building outline enhancement and extraction using iterative I0 smoothing and line enhancing. In *2019 IEEE International Conference on Image Processing (ICIP)*, 2019. 2
- [88] Cho-Ying Wu and Ulrich Neumann. Scene completeness-aware lidar depth completion for driving scenario. In *ICASSP*, 2021. 1
- [89] Cho-Ying Wu, Jialiang Wang, Michael Hall, Ulrich Neumann, and Shuo Chen. Toward practical monocular indoor depth estimation. In *CVPR*, 2022. 1, 2, 6
- [90] Cho-Ying Wu, Qiangeng Xu, and Ulrich Neumann. Synergy between 3dmm and 3d landmarks for accurate 3d facial geometry. In *2021 International Conference on 3D Vision (3DV)*, 2021. 1
- [91] Huaxiu Yao, Long-Kai Huang, Linjun Zhang, Ying Wei, Li Tian, James Zou, Junzhou Huang, et al. Improving generalization in meta-learning via task augmentation. In *ICML*, 2021. 3
- [92] Mingzhang Yin, George Tucker, Mingyuan Zhou, Sergey Levine, and Chelsea Finn. Meta-learning without memorization. In *ICLR*, 2020. 3
- [93] Wei Yin, Yifan Liu, Chunhua Shen, and Youliang Yan. Enforcing geometric constraints of virtual normal for depth prediction. In *ICCV*, 2019. 2
- [94] Wei Yin, Jianming Zhang, Oliver Wang, Simon Niklaus, Long Mai, Simon Chen, and Chunhua Shen. Learning to recover 3d scene shape from a single image. In *CVPR*, 2021. 1, 2, 5

- [95] Zehao Yu, Lei Jin, and Shenghua Gao. P²net: Patch-match and plane-regularization for unsupervised indoor depth estimation. In *ECCV*, 2020. 2
- [96] Weihao Yuan, Xiaodong Gu, Zuozhuo Dai, Siyu Zhu, and Ping Tan. New crfs: Neural window fully-connected crfs for monocular depth estimation. *CVPR*, 2022. 2
- [97] Zhenyu Zhang, Stéphane Lathuiliere, Andrea Pilzer, Nicu Sebe, Elisa Ricci, and Jian Yang. Online adaptation through meta-learning for stereo depth estimation. *arXiv preprint arXiv:1904.08462*, 2019. 3
- [98] Zhenyu Zhang, Stephane Lathuiliere, Elisa Ricci, Nicu Sebe, Yan Yan, and Jian Yang. Online depth learning against forgetting in monocular videos. In *CVPR*, 2020. 3
- [99] Yuyang Zhao, Zhun Zhong, Fengxiang Yang, Zhiming Luo, Yaojin Lin, Shaozi Li, and Nicu Sebe. Learning to generalize unseen domains via memory-based multi-source meta-learning for person re-identification. In *CVPR*, 2021. 3
- [100] Yiqi Zhong, Cho-Ying Wu, Suyu You, and Ulrich Neumann. Deep rgb-d canonical correlation analysis for sparse depth completion. In *Advances in Neural Information Processing Systems*, volume 32, 2019. 2
- [101] Junsheng Zhou, Yuwang Wang, Kaihuai Qin, and Wenjun Zeng. Moving indoor: Unsupervised video depth learning in challenging environments. In *CVPR*, 2019. 2